



Sedimentology, stratigraphy and geochemistry of a stromatolite biofacies in the 2.72 Ga Tumbiana Formation, Fortescue Group, Western Australia



J.M. Coffey^{a,1}, D.T. Flannery^{a,*}, M.R. Walter^a, S.C. George^{a,b}

^a Australian Centre for Astrobiology, School of Biotechnology and Biomolecular Sciences, University of New South Wales, New South Wales 2052, Australia

^b Department of Earth and Planetary Sciences, Macquarie University, New South Wales 2109, Australia

ARTICLE INFO

Article history:

Received 8 February 2013

Received in revised form 25 July 2013

Accepted 27 July 2013

Available online 7 August 2013

Keywords:

Pilbara

Stromatolites

Lacustrine

Neoproterozoic

Redmont

ABSTRACT

The 2.72 Ga Tumbiana Formation is a succession of clastic and carbonate rocks outcropping along the southern margin of the Pilbara Craton in Western Australia. It hosts abundant, diverse and exceptionally well-preserved stromatolites and has provided the setting for numerous investigations focussing on the Archaean biosphere. Despite its palaeobiological significance, the overall depositional setting of the Tumbiana Formation remains unclear. Here we present the results of stratigraphic, sedimentological and geochemical investigation of the Tumbiana Formation in the well-known Redmont/"Knossos" area and at several localities in the northwestern Pilbara sub-basin. We suggest these data are best explained by deposition in fluvial and lacustrine environments of an inward-draining continental basin. $\delta^{13}\text{C}_{\text{org}}$ values vary from -49.9‰ to -15.0‰ . Conical stromatolite morphologies, commonly attributed to cyanobacteria, are anomalously little depleted in $^{13}\text{C}_{\text{org}}$, implying a higher relative contribution of organic matter from phototrophic versus methane cycling metabolisms.

© 2013 Elsevier B.V. All rights reserved.

1. Introduction

The Fortescue Group is the basal member of the Mount Bruce Supergroup in Western Australia (Fig. 1), and overlies Paleoproterozoic basement rocks of the Pilbara Craton (Fig. 2). It was deposited between 2775 and 2630 Ma during a period of rifting and extensive volcanism (Thorne and Trendall, 2001; Blake et al., 2004). Flood basalts dominate the group, which also contains siliciclastic, volcanoclastic and carbonate units. Thorne and Trendall (2001) divided the Fortescue Group into four sub-basins: the northeast, northwest, Marble Bar and southern sub-basins.

The Tumbiana Formation of the Fortescue Group was deposited between subaerial lava flows of the underlying Kylena and overlying Maddina Formations. It was divided by Lipple (1975) into the Mingah Member, consisting predominantly of sandstones and subaerial lava flows with volcanoclastic and minor carbonate rocks, and the overlying Meentheena Carbonate Member, subsequently revised to Meentheena Member (Thorne and Hickman, 1998), consisting of dark, prominently outcropping stromatolitic limestone and recessive shale.

The age of the Tumbiana Formation is constrained by U–Pb zircon dates obtained from lavas in the Kylena Formation (2741 ± 3 Ma; Blake et al., 2004) and in the Maddina Formation (2717 ± 2 Ma; Nelson, 1998; Kojan and Hickman, 1999), and from detrital zircons recovered from Tumbiana Formation tuffaceous sandstones (2715 ± 6 Ma, Arndt et al., 1991; 2719 ± 6 Ma, Nelson, 2001; 2721 ± 4 Ma, Blake et al., 2004). Regional metamorphism was limited to prehnite–pumpellyite facies in the northeast, northwest and Marble Bar sub-basins, and to actinolite facies in the southern sub-basin (Smith et al., 1982).

Numerous studies have leveraged the low metamorphic grade and high-degree of preservation to study Neoproterozoic ecosystems from geochemical, isotopic and palaeontological perspectives. Previous investigations of the Meentheena Member have focused on the Meentheena area in the northeast sub-basin (Walter, 1983; Packer, 1990; Buick, 1992; Lepot et al., 2008; Awramik and Buchheim, 2009; Thomazo et al., 2009; Flannery and Walter, 2011), the Oakover Syncline in the northeast sub-basin (Buick, 1992; Van Kranendonk et al., 2006), the northwest sub-basin (Buick, 1992) and the area surrounding Redmont railway camp, including the site known colloquially as "Knossos" (Walter, 1983; Packer, 1990; Sakurai et al., 2005; Coffey et al., 2011).

Despite widespread renown as a repository of palaeobiological information, the overall depositional setting of the Tumbiana Formation remains problematic. The Mingah Member was interpreted as fluvial by Packer (1990), as fluvial and shallow marine

* Corresponding author. Tel.: +61 439742509.

E-mail address: dtf@unsw.edu.au (D.T. Flannery).

¹ Current address: Endeavor Operations Pty Ltd.

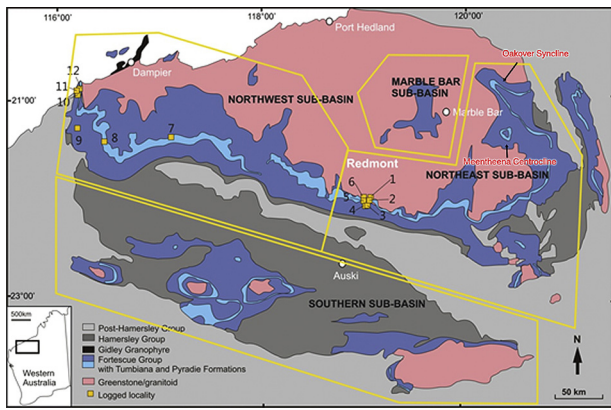


Fig. 1. Fortescue Group outcrop in the Pilbara Craton showing the localities logged for this study. (1) “Unconformity Hill”; (2) “Peacock Gorge”; (3) “Knossos”; (4) “Road Curve Gorge”; (5) “Campsite Hill”; (6) “Martin’s Hill”; (7) “Intersection Gorge”; (8) “Termite Mound Hill”; (9) “Ghost Cow Hill”; (10) “Mt. Potter South”; (11) “West Mt. Potter”; and (12) “North Mt. Rough”. Modified after Thorne and Trendall (2001).

by Thorne and Trendall (2001), and as alluvial and shallow marine by Sakurai et al. (2005). Interpretations of the Meentheena Member have also varied, with a marine setting favoured by Packer (1990), Thorne and Trendall (2001) and Sakurai et al. (2005), and a lacustrine interpretation advanced by Kriewaldt and Ryan (1967), Walter (1983), Buick (1992), Bolhar and Van Kranendonk (2007) and Awramik and Buchheim (2009). We attempt to address this problem through a study of the stratigraphy, sedimentology, geochemistry and palaeontology of the Tumbiana Formation in the Redmont/“Knossos” area.

2. Previous work

Walter (1983) noted abrupt lateral and vertical facies changes and abundant evidence for very shallow to periodically exposed conditions (prism cracks, wind generated ripple cross-lamination, tepee structures and intraclast grainstone) in the Meentheena Member in the Redmont/“Knossos” and Meentheena areas. A series of shallow ephemeral ponds and permanent lakes was proposed as being most consistent with these observations.

A marine setting for the Meentheena Member was favoured by Packer (1990), who studied widely spaced localities in the north-east Pilbara sub-basin. She described a recurring mid-succession



Fig. 2. Photo looking east from the “Martin’s Hill” locality. The Tumbiana Formation (white arrows) unconformably overlies the granite-greenstone basement in the background.

stromatolitic unit, tepee structures, intraclast “rosettes” (reworked tabular intraclasts) and an overlying fenestral limestone unit. A laterally uniform set of processes was inferred, such as that which commonly operates on a marine shoreline extending for hundreds of kilometres. This interpretation is supported by a general north to south thickening of the Tumbiana Formation into its southerly stratigraphic equivalent, the Pyradie Formation, first observed by Trendall and Blockley (1970).

Buick (1992) noted evidence for regular desiccation in the form of tepee structures and mud-cracks, which was interpreted as supportive of deposition in a periodically exposed, lacustrine setting. In addition, he noted the prevalence of scoriaceous (subaerial) basalt, widespread symmetrical (wind-generated) ripples, a lack of bidirectional current indicators and the unusual lack of gypsum casts, which are common features of younger marine or restricted saline environments (Sanz-Montero et al., 2009). Packer (1990) had previously reported gypsum casts, however, this report has not been confirmed by subsequent investigations. In any event, gypsum was probably a rare precipitate prior to the Great Oxidation Event (GOE).

Thorne and Trendall (2001) proposed a marine interpretation for the Meentheena Member. They noted that the Pyradie Formation consists of lithologies typical of a deeper shelf setting, including pillow lava, hyaloclastite, komatiite, minor chert and tuffaceous argillite, and interpreted the Tumbiana Formation as the shallower, northerly manifestation of a southerly-deepening marine paleogeography. A variation of this model was proposed by Sakurai et al. (2005), in which initial sedimentation included alluvial-fan deposits (the graded, ungraded and trough cross-stratified conglomerate at Redmont/“Knossos”) from late lowstand and early transgressive stages. The overlying sandstone and mudstone were interpreted as a series of transgressive and regressive shelf to coastal lithofacies successions. Sakurai et al. (2005) reported herringbone cross-stratification and desiccation cracks from the sandstone and mudstone facies. The report of herringbone cross-stratification was later questioned by Awramik and Buchheim (2009), who suggested this may have been a misinterpretation of trough cross-stratification. No herringbone cross stratification was observed in this study.

After performing a detailed stratigraphic and sedimentological study in the Meentheena area, Awramik and Buchheim (2009) considered a lacustrine setting most likely. They noted the prevalence of symmetrical ripples, desiccation cracks, stromatolites, distinctive geochemistry (see below), abrupt lateral and vertical facies changes and the cyclic nature of the lithofacies association (interpreted as representative of rapid water level fluctuations in a lacustrine setting).

Several additional studies have attempted to gain insights into the depositional setting of the Tumbiana Formation through geochemical analyses. The results of these analyses have been mixed, but have generally been interpreted as favouring a lacustrine setting. $\delta^{13}\text{C}_{\text{carb}}$ values reported by Walter (1983), Packer (1990) and Awramik and Buchheim (2009) are near zero. Packer (1990) suggested such values reflect a marine influence, whereas other authors have regarded the signal as inconclusive (Walter, 1983; Awramik and Buchheim, 2009). More recent analysis of drill core from both carbonate and fine siliciclastic units of the Tumbiana Formation has yielded $\delta^{13}\text{C}_{\text{carb}}$ values of -9.2 to 1.9% (Thomazo et al., 2009). $\delta^{18}\text{O}_{\text{carb}}$ values (-14.6 to -8.7% from drill core, -16.73 to -11.72% from outcrop samples) show a consistency across numerous studies (Schidlowski et al., 1983; Packer, 1990; Eigenbrode and Freeman, 2006; Awramik and Buchheim, 2009; Thomazo et al., 2009). Awramik and Buchheim (2009) also performed an analysis of $^{87}\text{Sr}/^{86}\text{Sr}$ values, which were found to fluctuate in accordance with cyclic lithofacies sequences. The values are dissimilar to and more variable than values reported from Archaean marine units (Veizer

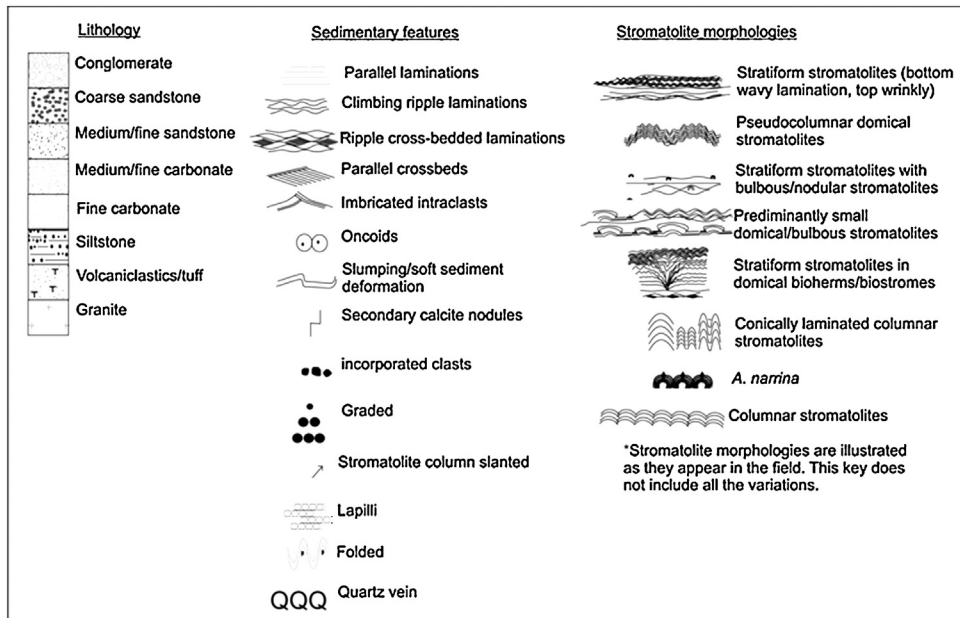
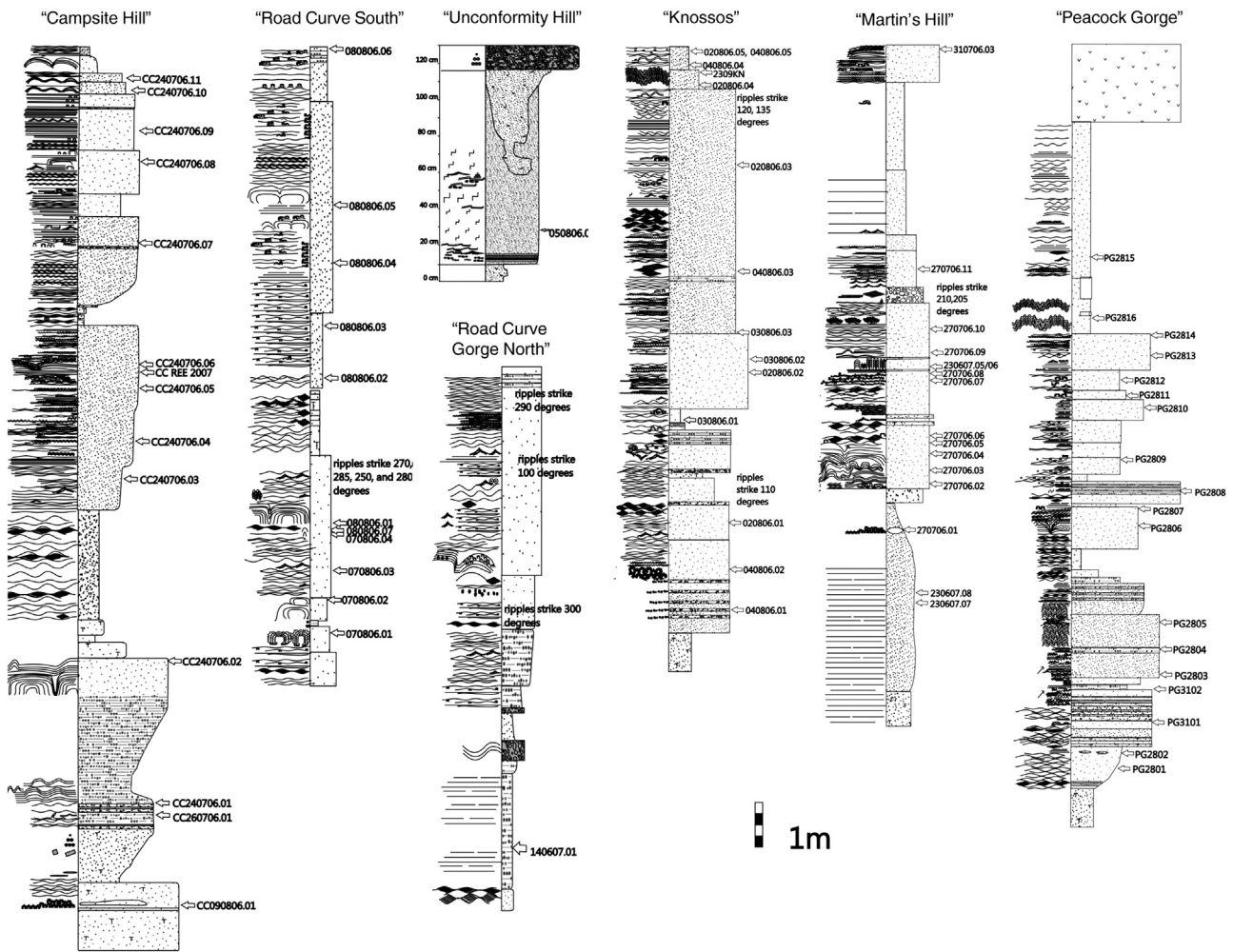


Fig. 3. Stratigraphic sections and samples logged at the Redmont/'Knossos' localities.

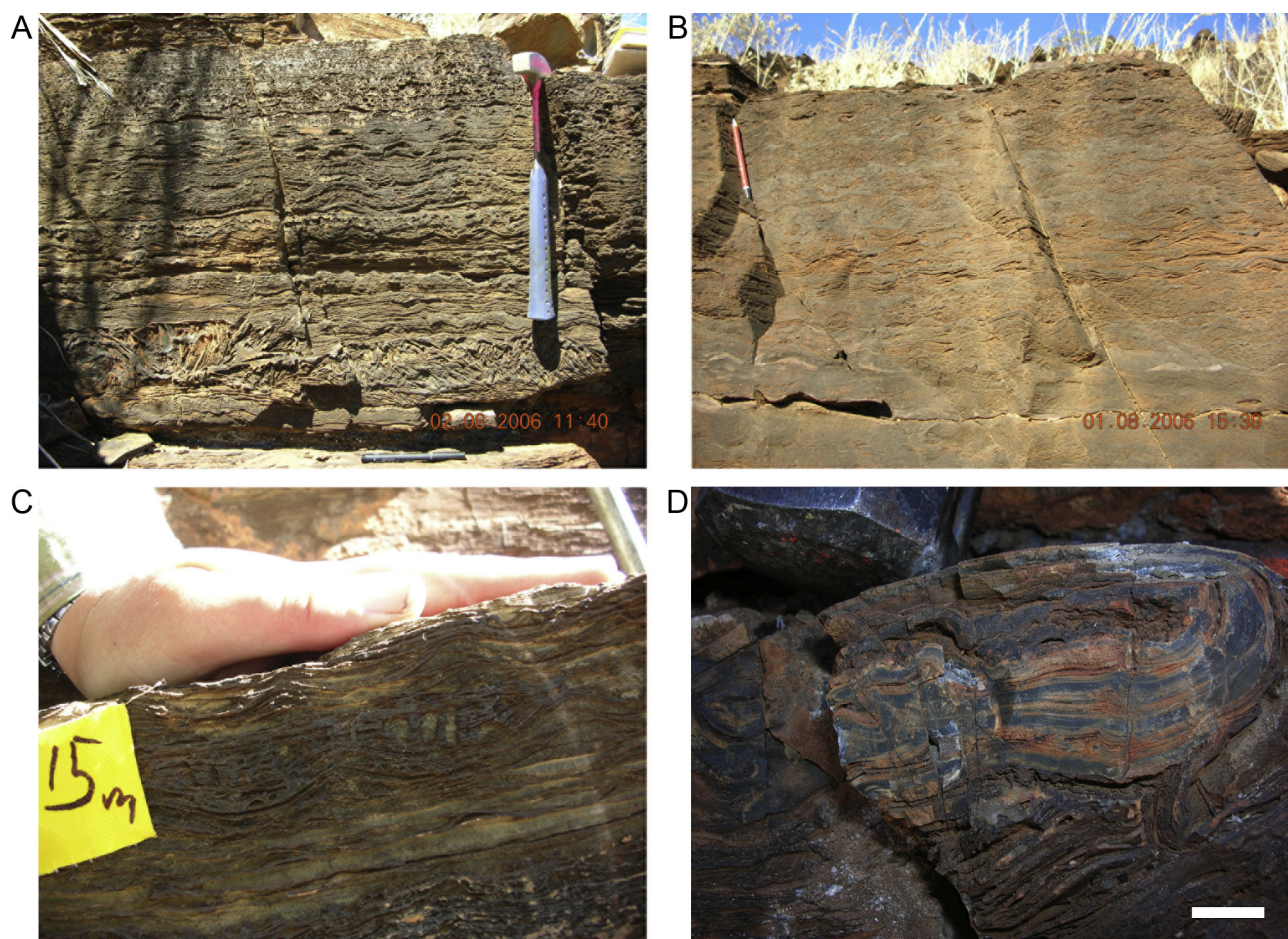


Fig. 4. Variability in stromatolite morphology. (A) Smooth and wavy-laminated stratiform stromatolites and imbricated intraclasts in a grainstone (below) at the “Knossos” locality. (B) A thick bed of ripple cross-laminated carbonate at the “Martin’s Hill” locality. (C) Columnar stromatolites nucleated on ripples at the “Road Curve Gorge” locality. (D) Finely laminated, partially silicified oncoids at the “Knossos” locality. Scale bar is 1 cm.

et al., 1989). Bolhar and Van Kranendonk (2007) reported the trace element geochemistry of carbonate from the Meentheena Member, interpreting their results as suggestive of a lacustrine signal, specifically, one incorporating a fluvial and/or “acidic lake signature”, or a very shallow lagoonal setting dominated by freshwater input.

3. Methods

Fieldwork was carried out by J.M. Coffey, M.R. Walter and S.C. George over two field seasons in 2006 and 2007. Investigations were confined to the northwestern Pilbara sub-basin (Fig. 1), an area largely neglected by previous studies, and the Redmont/“Knossos” area, the focus of several previous studies and debate in relation to the palaeoenvironment of the Tumbiana Formation (Walter, 1983; Packer, 1990; Buick, 1992; Sakurai et al., 2005).

Samples from the Tumbiana Formation were collected so as to obtain a range of stromatolite morphologies. Samples for geochemical analysis were further selected on the basis of avoiding detritus incorporated into stromatolite laminations, cross-cutting veins and proximity to tuffaceous material. A list of localities is provided in the supplementary material.

Potassium ferricyanide stain was used to distinguish dolomitic and calcitic carbonate, as described in Dickson (1965) and Lindholm and Finkelman (1972).

Trace element analyses were performed using a Thermo X-Series ICP-MS by Dr Balz Kamber, Laurentian University, Canada.

Instrument operating conditions and analytical procedures follow the protocol described in Lawrence et al. (2006). The instrument was calibrated using USGS geological reference materials W-2 and BHVO-1 and laboratory long-term average BHVO-2. More recently devised ‘Mud from Queensland’ (MUQ) normalisation is used in this study as it is thought to best represent Australian continental crust (Kamber et al., 2005).

$\delta^{13}\text{C}_{\text{carb}}$ and $\delta^{18}\text{O}_{\text{carb}}$ were analysed by C. Recio Hernández at the Stable Isotope Laboratory, University of Salamanca, Spain. The $\delta^{13}\text{C}_{\text{org}}$ data were obtained by A. Hill at the Centro de Astrobiología, Madrid. 50% HCl was reacted overnight to dissolve all carbonate in each powdered sample (~500 mg). The residues were rinsed to neutral with milli-Q water and oven-dried at 40 °C. The samples were run in continuous flow mode using a MAT253 mass spectrometer attached via a ConFloIII to a Thermo Flash HT elemental analyser. All analyses were run with two primary (i.e., international standards from the IAEA in Vienna) standards – USGS-24 (graphite) and NBS-22 (oil). Gas for $\delta^{13}\text{C}_{\text{carb}}$ was derived with 103% orthophosphoric acid. Corrections were made against the two standards using a 2-point normalisation procedure. At least two repeats were completed for each sample. The analytical precisions are $\pm 0.2\%$ for $\delta^{18}\text{O}_{\text{carb}}$ and $\delta^{13}\text{C}_{\text{carb}}$, and $\pm 0.3\%$ for $\delta^{13}\text{C}_{\text{org}}$.

4. New observations

The northwesterly units of the Tumbiana Formation are dominated by volcanoclastic rocks, sandstone, siltstone, mudstone and

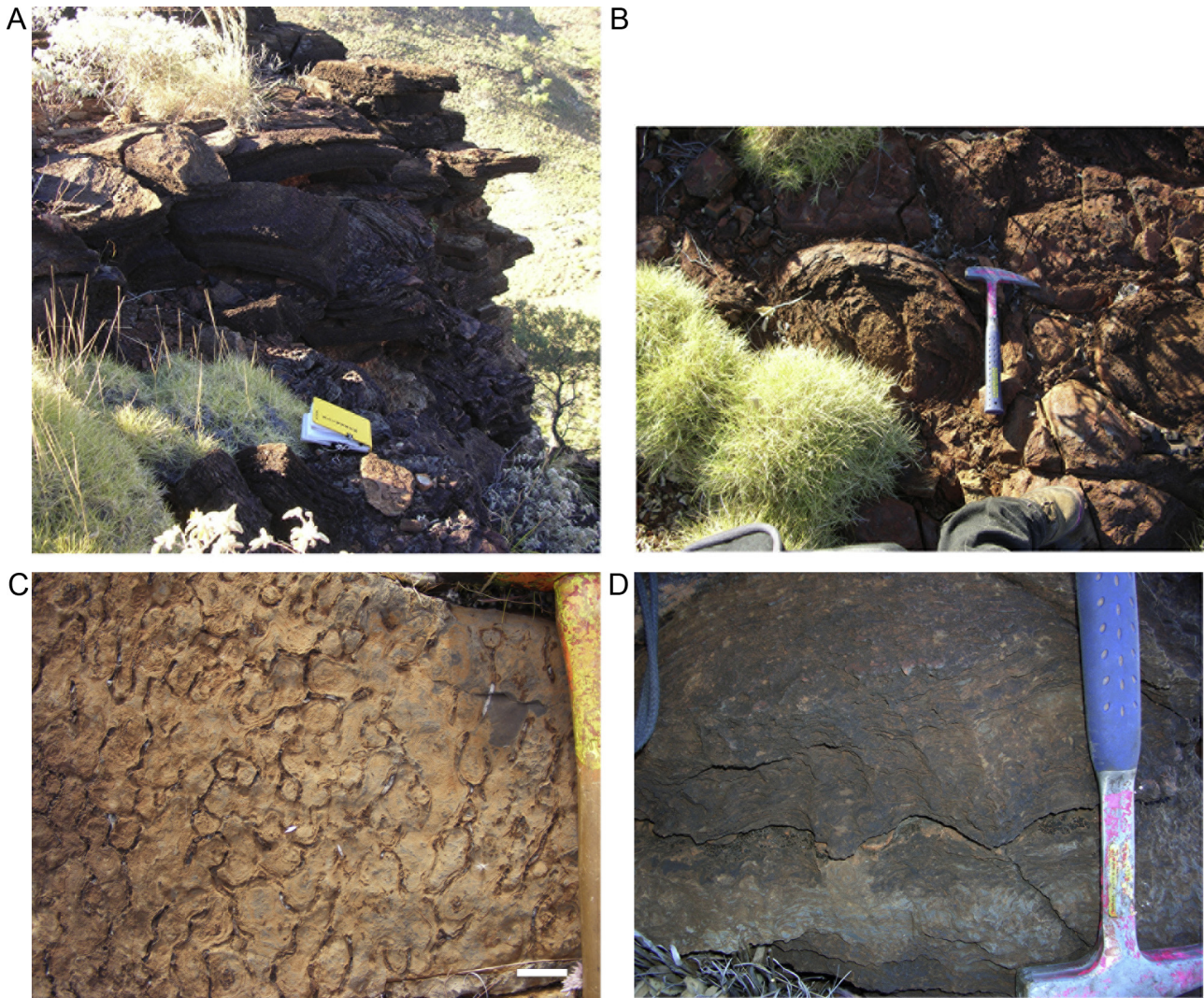


Fig. 5. Domical stromatolites in vertical section (A) and plan view (B) at the “Peacock Gorge” locality. (C) Plan view photograph showing the interlocking nature of domical stromatolites at the “Knossos” locality. Scale Bar is 5 cm. (D) Vertical section showing pseudocolumnar stromatolites at the “Peacock Gorge” locality.

thin, lenticular carbonate units. The Meentheena Member cannot be differentiated at most of these localities. In contrast, the Meentheena Member at Redmont/“Knossos” consists of relatively thick units of fine to medium grained carbonate, ripple cross-laminated calcareous sandstone, pebble conglomerate and finely laminated volcaniclastic units. Lateral correlation of carbonate units between the Redmont/“Knossos” area and localities logged in the northwest sub-basin was not possible (Fig. 3).

4.1. Northwesterly localities (Yarraloola and Pyramid 1:250,000 map sheets)

The Tumbiana Formation of the northwestern succession commonly lies conformably upon the Kylena Formation, which here consists of subaerial and subaqueous basaltic lava and volcaniclastic rocks (Thorne and Trendall, 2001). At all of the northwesterly localities, the Kylena Formation is overlain by 8–28 m of finely laminated, reworked and syndimentary volcaniclastic rocks and well-sorted, ungraded calcareous sandstone. Trough cross-bedding occurs in these basal units at “Termite Mound Hill”.

The “Mount Potter South”, “Termite Mound Hill” and “Intersection Gorge” sections contain 0.2–1 m of stromatolitic carbonate. Ripple cross-lamination and imbricated intraclasts are common

sedimentary features of this unit. Stromatolites are mostly stratiform and wavy-laminated biostromes and are less abundant here than at Redmont/“Knossos” and elsewhere in the formation. The “Intersection Gorge” locality has excellent specimens of the stromatolite *Alcheringa narrina* (Walter, 1972).

A unit of massive basalt (2–10 m) typically conformably overlies the volcaniclastic rocks, sandstone and/or carbonate. Thick units of lapilli-dominated tuff, basalt flows and coarse, well-rounded clastic grains within a fine grained matrix (heavily Fe-altered) continue the succession to the limit of outcrop. A thicker succession of volcanic rocks was logged at the “Termite Mound Hill” locality. Here, a scoriaceous pyroclastic unit (~1 m thick) continues the succession and is in turn capped by a finely laminated, 3 m thick, iron oxide-altered unit with climbing ripple cross-lamination and wavy laminations.

The more complete and well preserved successions of carbonate in the northwest sub-basin are nearer to the Redmont/“Knossos” area, such as the “Termite Mound Hill” and “Intersection Gorge” localities.

4.2. Redmont/“Knossos”

In the Redmont/“Knossos” area, the Mingah Member begins with tuffaceous conglomerate and sandstone deposited in the

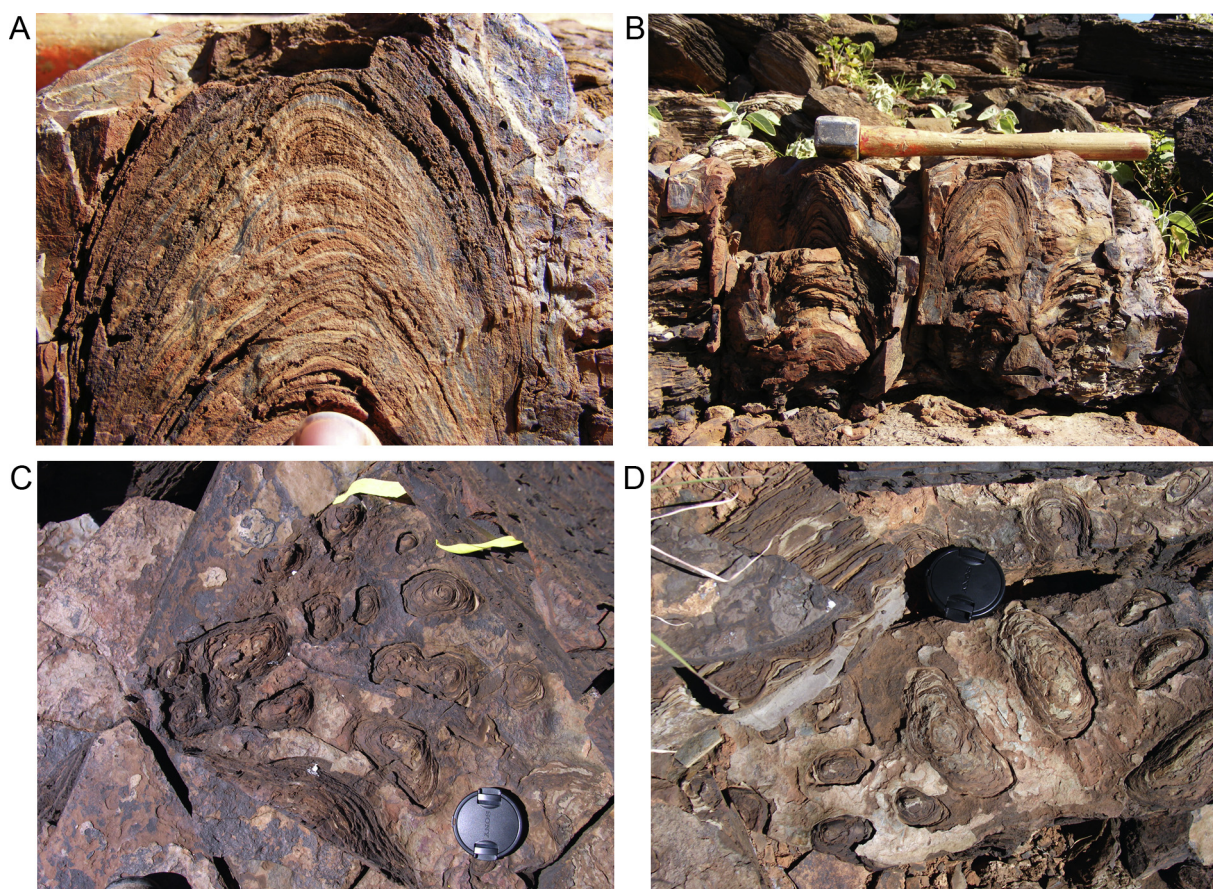


Fig. 6. Conically laminated columnar stromatolites at “Martin’s Hill” in cross section (A) and (B) and plan view (C) and (D).

topographic lows of basement rocks (Fig. 2). They are thickest in areas of low palaeotopography and thin out over higher relief areas of the undulating basement. Lenses of lapilli tuff are generally well sorted, ranging from thin laminations to graded, centimetre-scale beds and lenses of accretionary lapilli. Conglomerates consist of pebble to cobble-sized granite and quartz clasts within a fine-grained matrix. The conglomerate is ~14 m thick in the two most northerly localities and 1.5–2 m thick in the southerly localities. Angular to sub-angular clasts are up to 10 cm in diameter in the northerly localities and up to 1 cm in diameter at the southerly localities. The conglomerate is overlain by 3–24 m of reworked calcareous volcanoclastic rocks and quartz sandstone. Ripple cross-lamination is common in these sandy beds.

The major carbonate units are generally greater than 12 m thick and host a wide variety of stromatolite morphologies (Figs. 4–6). This is not the case at “Unconformity Hill”, where carbonate is limited to a 0.4 m, stromatolite-free unit with abundant soft sediment deformation features. An ooidal limestone rich in volcanic glass shards was observed at the base of the major carbonate unit at “Peacock Gorge”, where a sharp contact defines the top of this oolite and the bottom of a laminated mudstone. At “Campsite Hill”, the transition from the ripple cross-laminated volcanoclastic rocks, calcareous siltstone and sandstone to the major stromatolitic carbonate occurs with no obvious pre-depositional erosion, although a disconformity was observed at “Martin’s Hill”. Units hosting stromatolites are dominantly fine grained carbonate, with thick beds of ripple cross-laminated sandstone (Fig. 4A) and thin volcanoclastic interlaminae occurring throughout the major carbonate unit. Imbricated intraclasts [including examples reworked into “rosettes”, see Ricketts and Donaldson (1979), Packer (1990) and

Awramik and Buchheim (2009)] and oncoids are common sedimentary features.

A lower carbonate unit occurs in the two north-western localities (“Martin’s Hill” and “Campsite Hill”). It occurs as small lenses in laminated, calcareous volcanoclastic rocks and siltstone ~10 m below the main carbonate unit. The overlying unit of volcanic tuff contains thick (>0.5 m) beds of climbing symmetrical ripple cross-lamination and ripple cross-laminated volcanoclastic sandstone.

The contact between stromatolitic carbonate and overlying basalt of the Maddina Formation is conformable where logged.

4.3. Stromatolitic biofacies assemblages

Stromatolitic features are described below using the terminology of Glaessner et al. (1969), Hofmann (1969) and Walter (1972).

Very fine-grained carbonate constitutes the majority of the stromatolitic units. Stromatolitic laminae consist predominantly of neomorphic micrite with minor siliciclastic and volcanoclastic detrital components (Fig. 7), which also comprise the majority of inter-stromatolite fill. Ferroan dolomite could not be distinguished from ferroan calcite by use of the potassium ferricyanide stain; however, X-ray diffraction analysis suggests stromatolitic carbonate is composed predominantly of calcium carbonate and SiO₂ (volcanic tuff and silicified laminae).

Four biofacies interpreted as representing shallow subaqueous environments are dominated by stratiform stromatolites, small bulbous stromatolites (including *A. narrina*), columnar stromatolites and pseudocolumnar stromatolites in domical bioherms

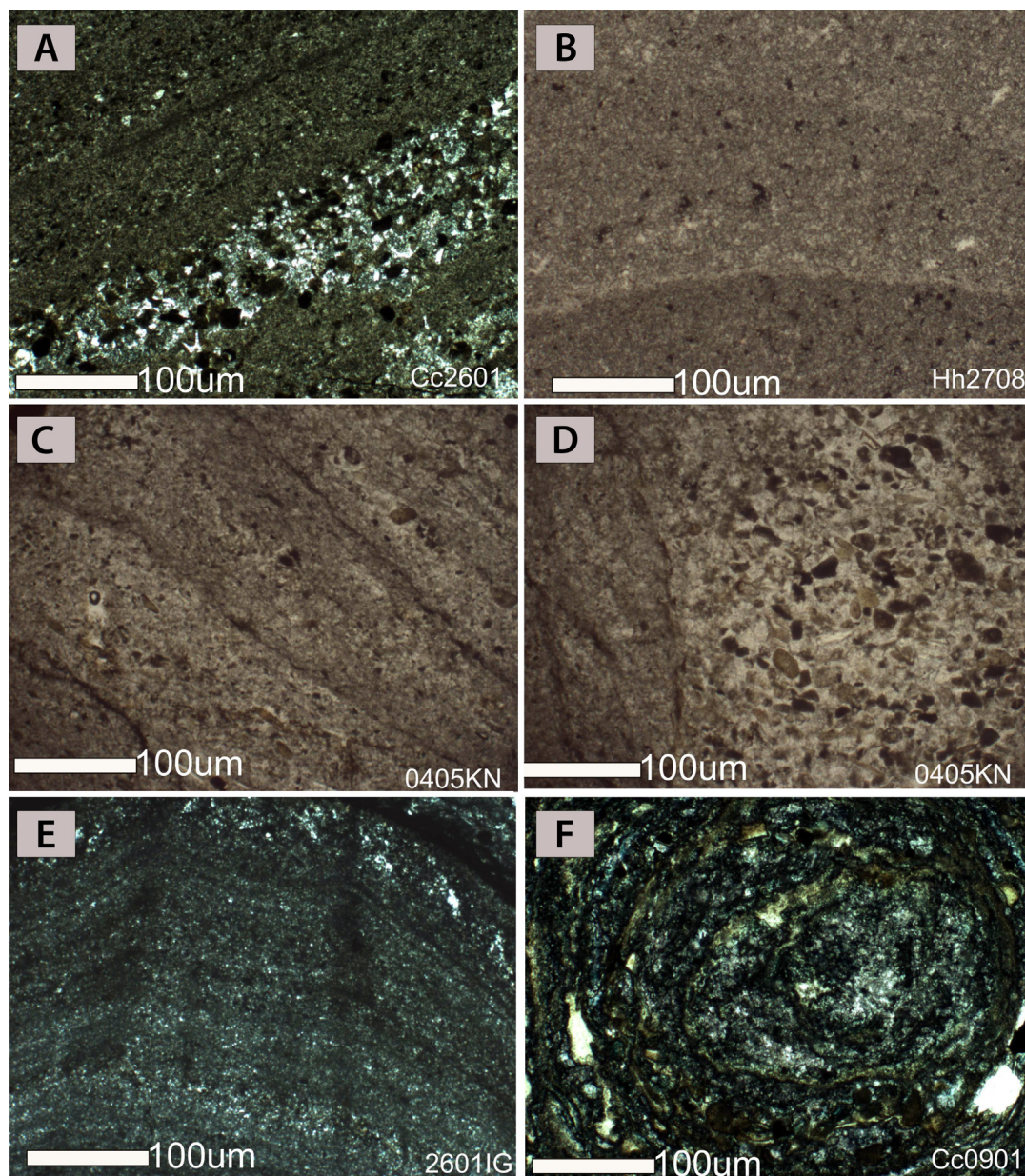


Fig. 7. Thin section photomicrographs of Meentheena Member stromatolites taken in plane polarised light. (A) Tuffaceous debris comprising laminations within a smooth, stratiform dome. (B) Faint laminae within a conically laminated stromatolite. (C) Pseudocolumnar stromatolites within a bioherm which have incorporated detrital material in the paler laminae. (D) Contact between a pseudocolumn and detrital infill. (E) The apex of a bulbous/nodular stromatolite. (F) Plan view of a small nodular/bulbous stromatolite.

(Figs. 5 and 6). Deeper facies include conically laminated columnar stromatolites and large, smooth to wrinkly, domical bioherms in finer-grained carbonates. Stromatolites in the study areas are typically elongate along an east–west axis (Fig. 8).

The majority of the stromatolitic successions begin with a basal unit of ripple cross-laminated carbonaceous sandstone. A pebble conglomerate (~0.5 m thick) occurs within the stromatolitic carbonate at “Martin’s Hill”. The conglomerate contains sub-rounded clasts, mostly ungraded, and occurs as 2–5 cm alternating planar cross-beds of pebble and coarse sandstone. This is overlain by stromatolitic carbonate which continues up to the limit of outcrop.

We identify three major transgressive events (Figs. 9 and 10), marked at their peaks by high synoptic relief, wide-diameter bioherms and domical stromatolites (Fig. 5), as well as distinct geochemical signatures (Fig. 11).

4.3.1. Stratiform stromatolites

Stratiform stromatolites are distinguished by smooth, wavy or wrinkly laminations and occur in tabular bioherms and biostromes (Fig. 4A). Imbricated intraclasts (“rosettes”) commonly occur alongside these laminations and are frequently draped by new laminae. Stratiform stromatolites commonly encapsulate small domed biostromes. Oscillations of laminae occur with wavelengths of 1–5 cm and resemble symmetrical ripple cross-lamination.

4.3.2. Centimetric domical stromatolites

Centimetre-scale domical stromatolites are characterised by laminae peaking near the central point of the stromatolite. They correspond to *A. narrina* (Walter, 1972), although this biofacies also includes other small nodular/bulbous stromatolites. Laminae are typically smooth, but may also be wavy with low to no inheritance. Large numbers of individuals occur together and commonly

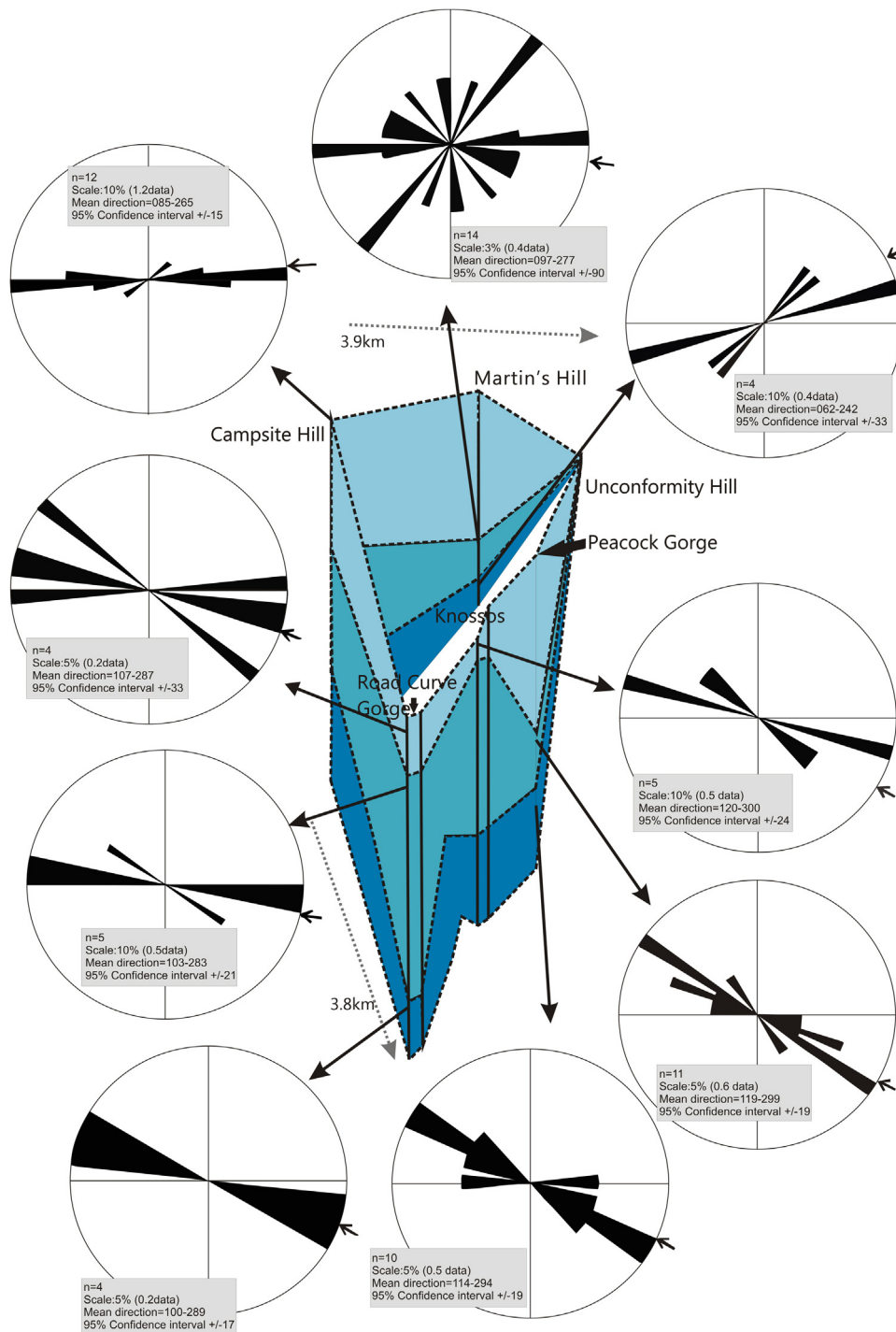


Fig. 8. Direction of elongation of stromatolites including bioherms/biostromes at the Redmont/'Knossos' localities. Arrows indicate the relative position in the succession where features were measured. No data were available for 'Unconformity Hill'. Plotted using GEORINT.

nucleate on uneven surfaces, such as imbricated intraclasts. These small stromatolites and stratiform stromatolites are the only two biofacies to occur in the westerly localities of the northwest sub-basin.

4.3.3. Columnar stromatolites

Columnar stromatolites are generally less than 10 cm high, 1 cm wide, and possess very little synoptic relief. They are finely laminated and display occasional bridging across wide infill areas. Columns are erect and uniform with no branching. Lamina shapes

range from gently to moderately convex to rhombic. Columns are not abundant and occur in small clumps and bioherms.

4.3.4. Pseudocolumnar bioherms

Sub-spherical bioherms of pseudocolumnar stromatolites are up to 90 cm in height with up to 20 cm of synoptic relief (Fig. 5). Laminae are smooth and locally bridge between columns. This biofacies is frequently overlain by ripple cross-laminated volcaniclastic sediment.

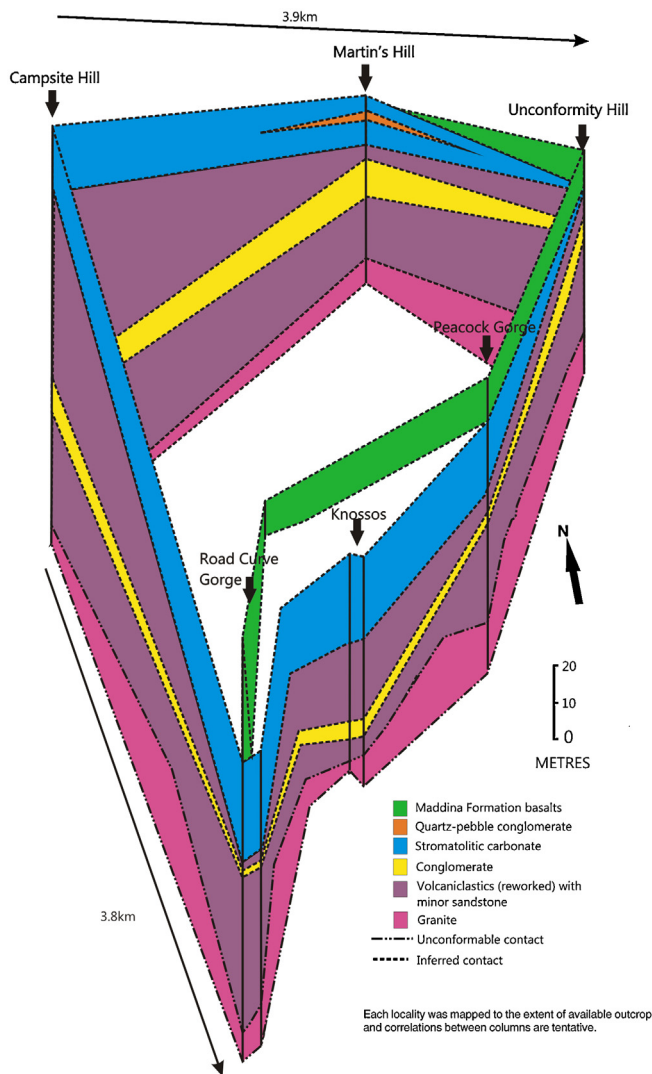


Fig. 9. Three dimensional fence diagram showing major lithological units in the Redmont/'Knossos' area.

4.3.5. Conically laminated columnar stromatolites

Conically laminated columnar stromatolites occur midway through the carbonate succession at the "Martin's Hill" locality. They can be traced laterally for ~100 m, however, towards the limits of current outcrop the columns appear increasingly stubby and less numerous. They possess the axial zones diagnostic of *Conophyton*, a group of conical stromatolites whose morphologies are often attributed to biological influences (Maslov, 1938; Donaldson, 1976; Schopf and Sovietov, 1976; Walter et al., 1976; Jones et al., 2002; Petroff et al., 2010; Shepard and Sumner, 2010; Flannery and Walter, 2011).

Individuals are 2–40 cm high and possess conical laminae with a shifting axial zone, uneven column margins and no branching (Fig. 6A and B). Macro-lamination visible in outcrop relates to the presence of thin, silicified laminae separating thicker areas of neomorphic micrite. Detritus occurs in areas of inter-stromatolite fill and in stromatolitic laminae, especially in lower-relief bridging laminae. Individuals appear to be roughly equally spaced in plan view exposures (Fig. 6C and D). Surrounding sediments consist of calcilitite to calcisiltite lacking the shallow water sedimentary features reported from the other facies. We infer a deeper water setting for this facies, which accords with similar interpretations for the setting of Proterozoic occurrences of *Conophyton* (e.g., Donaldson, 1976).

4.4. Trace element geochemistry

Full trace element data are presented in the Supplementary material. Equations used to calculate elemental anomalies are after Lawrence and Kamber (2006) and are given in the Supplementary material. Trace elemental analyses are presented according to locality, the relative position of the sample within the major carbonate unit (Fig. 11) and stromatolite morphology (Fig. 12).

Carbonate samples of the Tumbiana Formation are characterised by an expression of light rare earth element (REE) depletion, demonstrated by the ratios $Pr/Yb_{MUQ} = 0.8 \pm 0.5$, $Pr/Sm_{MUQ} = 0.9 \pm 0.2$ and $Sm/Yb_{MUQ} = 0.8 \pm 0.4$, with near zero Eu anomalies ($Eu/Eu^*_{MUQ} = 0.9 \pm 0.3$). La and Gd display no to slight positive anomalies ($La/La^*_{MUQ} = 1.2 \pm 0.2$; $Gd/Gd^*_{MUQ} = 1.0 \pm 0.2$). No anomalous normalised concentrations are observed for Ce. Y/Ho ratios remain consistent at 28.3 ± 2.4 . All concentrations range over one order of magnitude (Figs. 11 and 12).

Collectively, carbonate samples from all the northwesterly localities display similar signatures with expressions of light REE depletions and no Eu or Ce anomalies (Fig. 11A). Carbonate samples from the Redmont/'Knossos' locality show no enrichments in Eu or Ce, but have slight changes in preference for light, middle or heavy REE depletion (Fig. 11B). Carbonate is for the most part lacking in anomalies typically associated with marine depositional environments (Webb and Kamber, 2000), although there is some inhomogeneity across sections measured at Redmont/'Knossos'.

There is evidence of slight water chemistry changes between samples. We observed a trend from consistent light REE depletion in the lower parts of the carbonate unit to middle and heavy REE depletion moving upwards through the section (Fig. 11C–E). This is shown by the Pr_{MUQ}/Er_{MUQ} ratio, which is 0.633–0.818 in the basal carbonate unit, and also in all the westerly samples, 0.445–0.685 in the mid-carbonate unit, and 0.897–1.185 in the upper carbonate unit.

The MUQ-normalised patterns for samples collected from bulbous stratiform stromatolites (Fig. 12A and D) and *A. narrina* (Fig. 12B and E) typically display light REE depletion, although one *A. narrina* sample has middle REE enrichment (Fig. 12E). Pseudocolumnar stromatolites (Fig. 12C and F) display an enrichment of light REE with some negatively anomalous Eu, and conically laminated columnar stromatolites (Fig. 12G) are light REE depleted, with some Eu depletion.

The western-most sample (1704TM) from "Termite Mound Hill" demonstrates a significant Eu anomaly, possibly indicating hydrothermal activity. Other potential sources of a Eu anomaly include underlying units such as the Lyre Creek Member of the Hardey Formation. However, at this locality the Lyre Creek Member does not underlie the Tumbiana Formation (Kojan and Hickman, 1999), and a Lyre Creek Member source for the signature is unlikely.

4.5. Stable isotope geochemistry

The details of 48 carbon and oxygen isotope measurements obtained from 31 carbonate samples are listed in the Supplementary material and shown in stratigraphic context in Fig. 13.

$\delta^{13}C_{carb}$ values range from -8.30‰ to $+1.13\text{‰}$ (mean = -0.76‰ , standard dev. = 1.77‰).

$\delta^{13}C_{org}$ values range from -49.9‰ to -15.0‰ (mean -43.4‰ , standard dev. = 8.09‰). Stromatolites are strongly depleted in $^{13}C_{org}$ (Fig. 14), the only exception being the conically laminated columnar stromatolites which are relatively enriched (-16‰). $\delta^{18}O_{V-PDB}$ values are highly depleted (-23.4‰ to -13.7‰ , mean -18.0‰ , standard dev. = 1.78‰), suggestive of diagenetic overprinting, however, no consistent correlation between $\delta^{13}C_{carb}$ and $\delta^{18}O_{carb}$ is present. The co-efficient of correlation for all

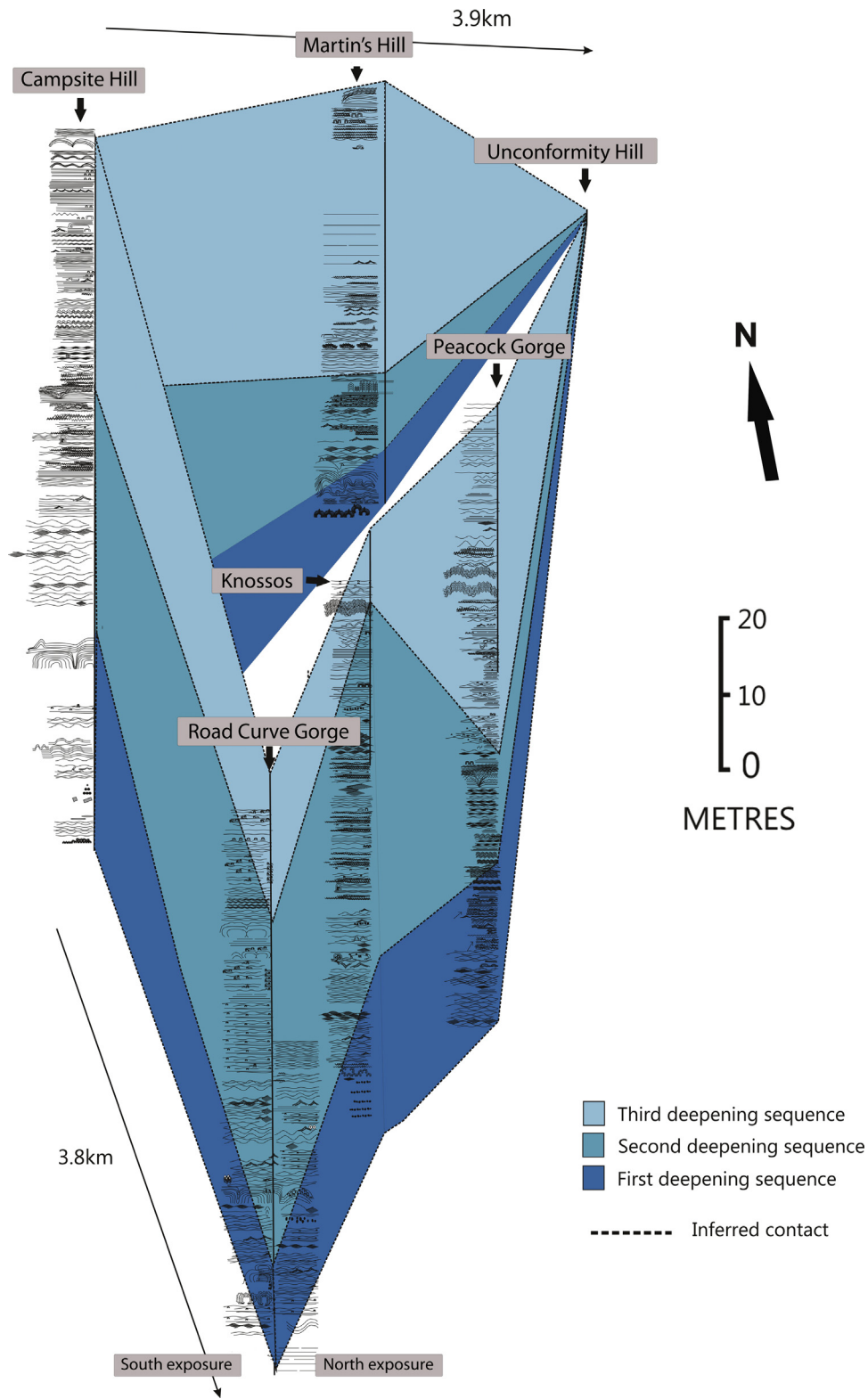


Fig. 10. Fence diagram showing the three transgressive events interpreted for the major carbonate unit in the Redmont/'Knossos' area.

localities is 0.44, slightly higher than that reported by Awramik and Buchheim (2009) for Meentheena Member carbonate. When data are restricted to the Redmont/'Knossos' and northwesterly localities, the correlation coefficients are 0.17 and 0.90, respectively. There is no clear correlation of $\delta^{18}\text{O}$ with facies changes.

5. Discussion

It is possible that parts of the Tumbiana Formation were deposited under marine conditions, as has previously been suggested (Packer, 1990; Thorne and Trendall, 2001; Sakurai et al., 2005). However, in this and in previous studies, no definitive

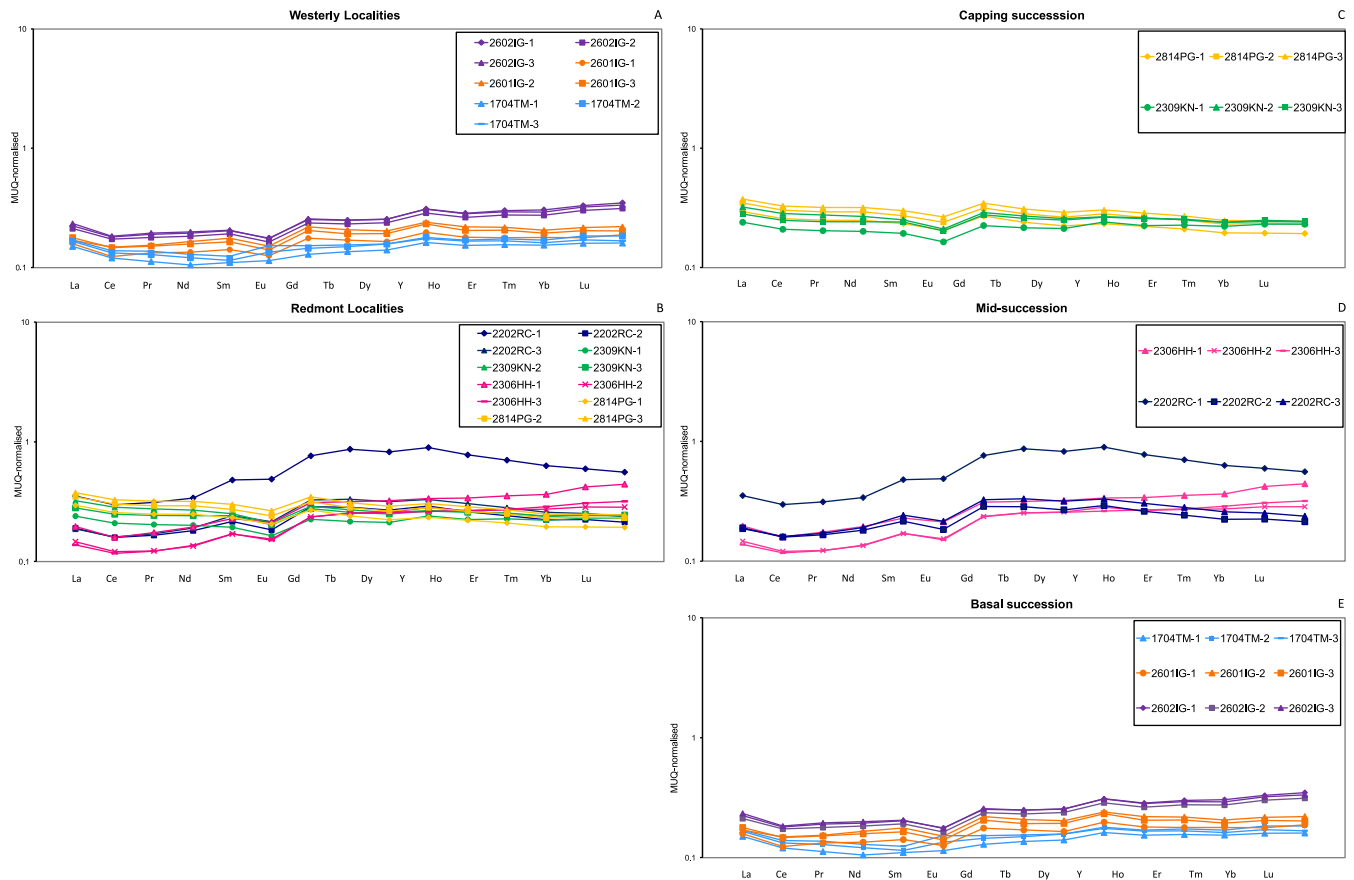


Fig. 11. MUQ-normalised REE concentrations of carbonates grouped according to northwesterly (A) and Redmont/"Knossos" (B) localities, and by their relative position within the major carbonate unit (C–E).

marine sedimentary features have been found in the Meentheena Member, despite the presence of extensive outcrop and considerable, long-standing interest in the unit. Due to the absence of paleoenvironmentally diagnostic fossils in rocks of this age, a lacustrine setting is also difficult to establish. We thus base our paleoenvironmental interpretation upon the balance of probabilities through careful consideration of the circumstantial evidence.

The conglomerate at Redmont/"Knossos" is most consistent with debris flows associated with an aggrading alluvial fan, as has been suggested by Sakurai et al. (2005). The bed thickness and clast size distribution suggest the fan was aggrading in a southerly direction. We find no marine sedimentary features in the overlying channelised sandstone and suggest it was deposited in a braided river system. Stromatolites elongated along an E–W axis are parallel to the orientation of crests of (wind-driven) symmetrical ripples and are not associated with current-generated sedimentary features. The three transgressive events recorded in the carbonate units cannot be correlated laterally with westerly localities or with the Meentheena area to the east, where Awramik and Buchheim (2009) reported as many as 25 transgressive and regressive events. Abrupt lateral and vertical facies changes in the carbonate unit at Redmont/"Knossos" and the broader non-correlation of northwesterly, Redmont/"Knossos" and Meentheena area carbonate units is typical of lacustrine settings (Platt and Wright, 2009). This, along with the prevalence of subaerial lava (indicative of prolonged subaerial exposure) and the absence of marine sedimentary features, suggest Meentheena Member carbonate rocks may represent a series of disconnected, ephemeral lakes associated with the distal

elements of an inward draining continental basin (cf. Nichols and Fisher, 2007). Further work focussing on paleocurrent readings and the stratigraphy and sedimentology of the underlying Mingah Member is required. Air-fall tuff, lava flows and accretionary lapilli indicate volcanism continued during deposition of the unit.

Although dominated by patterns of light REE enrichment, the trace element geochemistry is inconclusive, as more marine-like signatures (middle and heavy REE depletion; cf. Webb and Kamber, 2000) are also seen, particularly in the upper beds of the major carbonate unit. This may indicate a transition from freshwater-dominated to estuarine conditions midway through the succession. Notwithstanding this, we note that in the absence of associated Y and Gd anomalies, these data provide only a weak indication of marine conditions. The Y/Ho ratios are slightly supra-chondritic (average = 30.5), low in comparison to those recorded from known marine palaeoenvironments (Y/Ho ~ 60; Lawrence et al., 2006), yet within the range of previously reported values for the Fortescue Group (20–35) and of lacustrine stromatolites of the Eocene Green River Formation (29), as measured by Bolhar and Van Kranendonk (2007). The lack of significant Ce anomalies suggests the wider environment did not allow for the oxidation of Ce (Bau and Alexander, 2006). Overall, the REE + Y signals are likely of primary origin; correlations between $\text{Eu}/\text{Eu}^*_{\text{MUQ}}$ and $\text{REE}/\text{REE}_{\text{MUQ}}$ have previously been used (e.g., in Bolhar and Van Kranendonk, 2007) to infer samples have not been affected by secondary processes such as groundwater movement, and we find similar correlations here. Moreover, the correlation of Sr and U to Y/Ho in stromatolitic carbonate free of detrital material is also

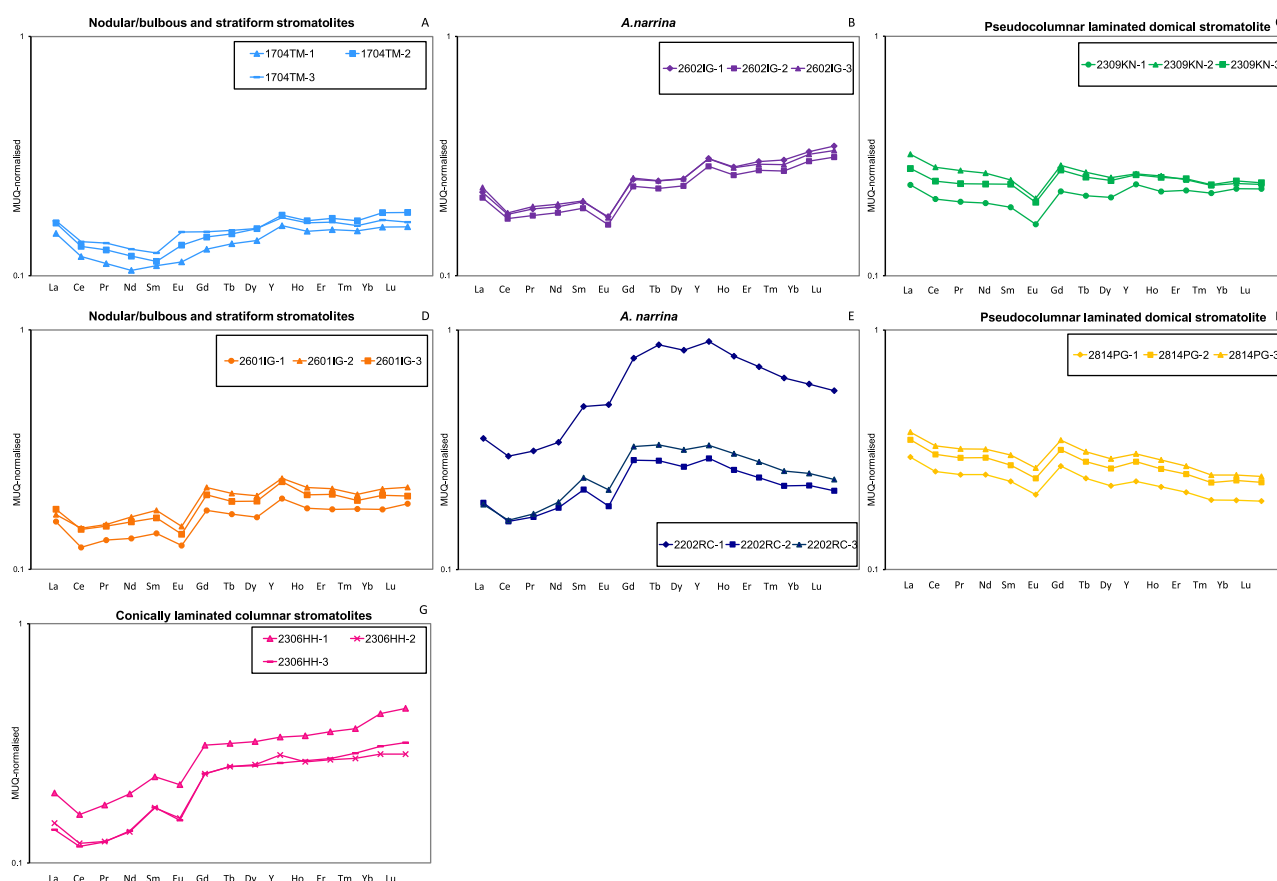


Fig. 12. MUQ-normalised REE concentrations grouped according to stromatolite morphology. Stratiform and bulbous stromatolites (A) and (D). *A. narrina* (B) and (E). Pseudocolumnar stromatolites in domical bioherms (C) and (F). Conically laminated columnar stromatolites (G).

suggestive of insignificant mixing with groundwater. The elevated light REEs in micritic stromatolitic laminae are consistent with results obtained from Proterozoic precipitated stromatolites (Corkeron et al., 2012).

Dolomite is a typical lithology of ancient marginal marine carbonates where it is often thought to record the former presence of saline waters with low Ca/Mg ratios. The paucity of dolomite in the Meentheena Member, in contrast to the dolomitic mineralogies of other marine Archaean units, including Fortescue Group units within the same sub-basin (cf. the Mopoke Member, Kylena Formation) can be accounted for by freshwater input associated with a lacustrine setting. Similarly, aragonite fans and Mg-calcite seafloor crusts are also absent from the Meentheena Member, but are common components of other Archaean and Paleoproterozoic marine units (Grotzinger and James, 2000), even within the same sub-basin and group (Flannery et al., 2012).

$\delta^{13}\text{C}_{\text{carb}}$ values vary with no predictable pattern throughout the carbonate succession, suggesting they are likely primary. However, some westerly localities may be significantly overprinted. They exhibit a positive co-variance between $\delta^{18}\text{O}$ and $\delta^{13}\text{C}$, a feature known to indicate alteration by meteoric waters (Allan and Matthews, 1982). In modern lakes, changes in $\delta^{18}\text{O}_{\text{carb}}$ values to within 5‰ can be the result of temperature/water depth fluctuations (Holmes et al., 2010). Other studies of modern lakes have shown $\delta^{18}\text{O}_{\text{carb}}$ values to vary with salinity and distance to the mouths of major rivers, due to variations in evaporation rates and freshwater input (e.g., Liu et al., 2009).

The highly depleted $\delta^{13}\text{C}_{\text{carb}}$ values reported here are in contrast to the values clustering around 0‰ reported by Awramik and Buchheim (2009) from the Meentheena area and by other authors (Walter, 1983; Packer, 1990) from the northeast sub-basin, and are similar to more-variable values reported from northeast sub-basin drill core (Thomazo et al., 2009). Our highly depleted $\delta^{13}\text{C}_{\text{carb}}$ values may be indicative of methane oxidation resulting in depleted bicarbonate, or possibly of a more acidic local environment (Abell et al., 1982), potentially due to nearby volcanic activity or to the neutralisation of a saline environment.

Wide ranging $\delta^{13}\text{C}_{\text{org}}$ values obtained from shallow water stromatolitic carbonates are comparable to values obtained by Eigenbrode and Freeman (2006) from Tumbiana Formation drill core, and by Walter (1983) and Packer (1990) from outcrop. Eigenbrode and Freeman (2006) interpreted a bimodal distribution of $\delta^{13}\text{C}_{\text{org}}$ values in Neoproterozoic units of the Hamersley Group as representing the presence of mixed methane-cycling and photosynthetic microbial communities in shallow-water facies, and communities dominated by methane-cycling metabolisms in deeper-water facies. The anomalously less depleted $\delta^{13}\text{C}_{\text{org}}$ samples from the “Martin’s Hill” locality support this hypothesis, as this biofacies alone contains stromatolite morphologies commonly associated with *Conophyton* and a structurally dominant component of phototrophic bacteria (e.g., Schopf and Sovietov, 1976; Walter et al., 1976; Jones et al., 2002; Petroff et al., 2010; Shepard and Sumner, 2010; Flannery and Walter, 2011).

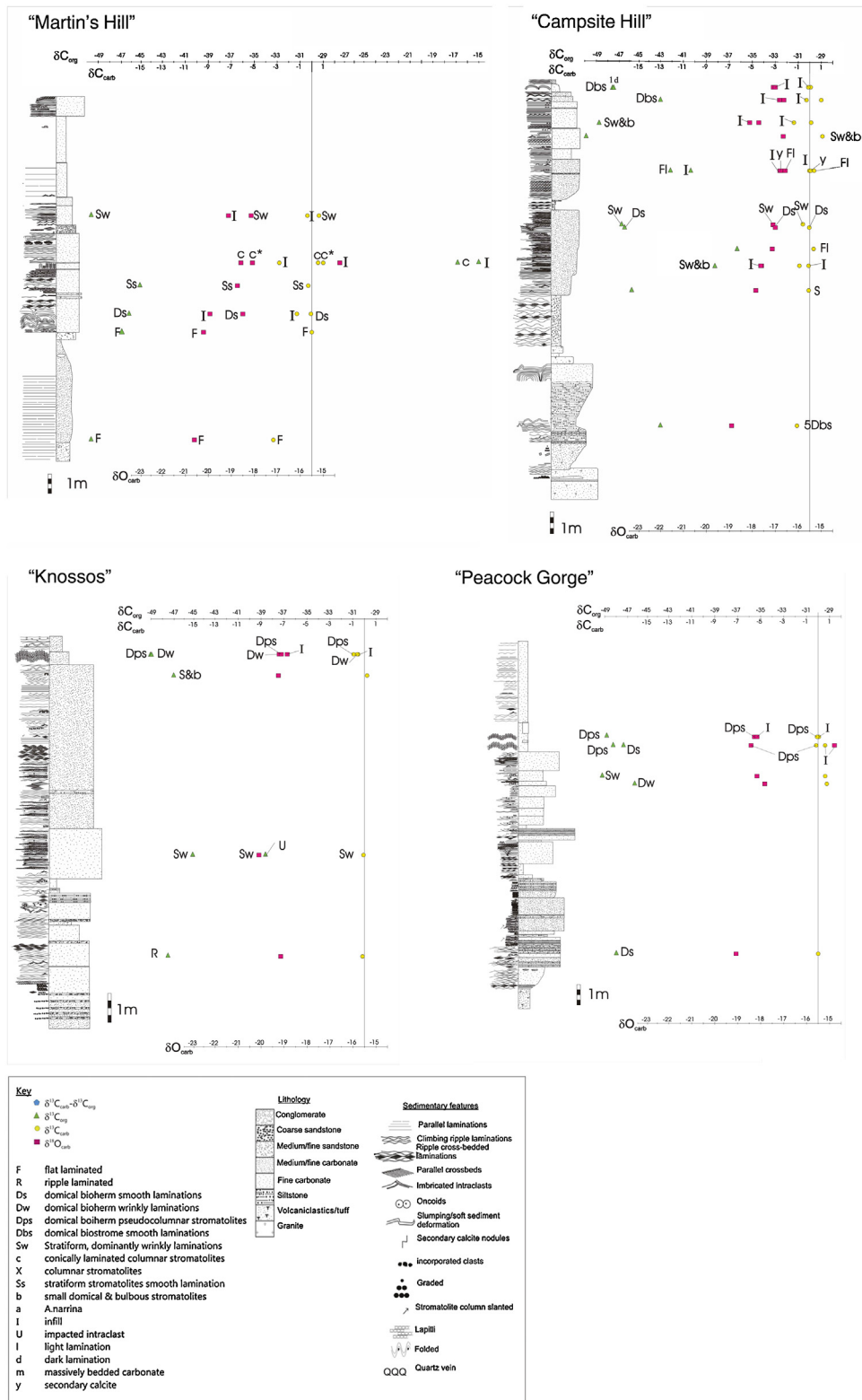


Fig. 13. Stratigraphic sections and stable isotope data logged in the Redmont/“Knossos” area.

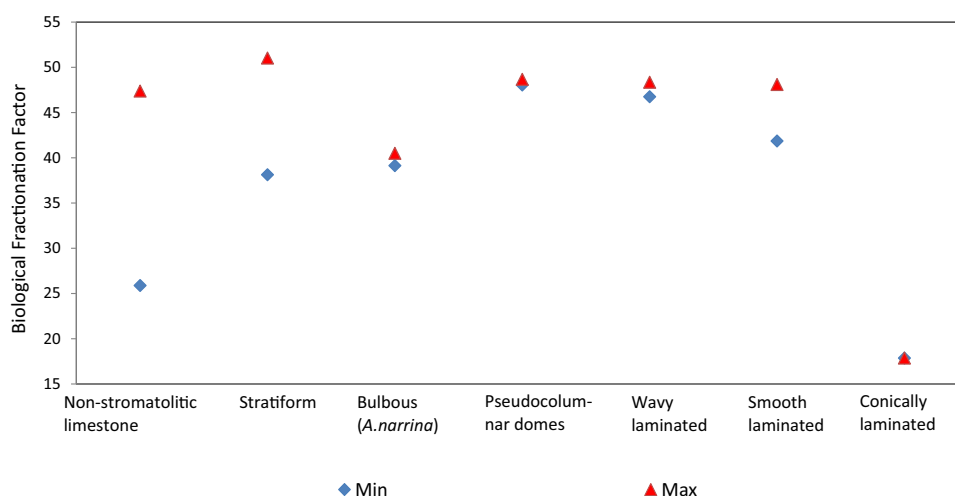


Fig. 14. Biological fractionation factor ($\delta^{13}\text{C}_{\text{carb}} (\text{‰}) - \delta^{13}\text{C}_{\text{org}} (\text{‰})$) arranged left to right according to inferred increasing water depth of stromatolites facies.

6. Concluding remarks

The carbon isotope evidence suggests the operation of an active biological methane cycle during deposition of Tumbiana Formation stromatolites. Evidence from carbon isotopes and stromatolite morphologies suggests a phototrophic metabolism may have been more important in shallow water stromatolites that are relatively enriched in $^{13}\text{C}_{\text{org}}$. The stratigraphic, sedimentological and geochemical data are most consistent with the interpretation that the carbonate units of the Meentheena Member were deposited in a series of shallow, ephemeral lakes.

Acknowledgements

We thank the Geological Survey of Western Australia for generous logistical field support and scientific assistance, particularly from Kath Grey and Arthur Hickman. Andrew Hill from Centro de Astrobiologia is thanked for assistance with isotope analysis. J.M.C. acknowledges support from an ARC grant to M.R.W., and from the Australian Centre of Astrobiology. D.T.F. is supported by an Australian Government Postgraduate Award. M.R.W. acknowledges the Australian Research Council for a Discovery Grant and a Professorial Fellowship. S.C.G. acknowledges the Australian Research Council for funding. We thank two anonymous reviewers who helped improve the manuscript.

Appendix A. Supplementary data

Supplementary data associated with this article can be found, in the online version, at <http://dx.doi.org/10.1016/j.precamres.2013.07.021>.

References

- Abell, P.I., Awramik, S.M., Osborne, R.H., Tomellini, S., 1982. Plio-Pleistocene lacustrine stromatolites from Lake Turkana, Kenya; morphology, stratigraphy and stable isotopes. *Sediment. Geol.* 32, 1–26.
- Allan, J.R., Matthews, R.K., 1982. Isotope signatures associated with early meteoric diagenesis. *Sedimentology* 29, 797–817.
- Arndt, N.T., Nelson, D.R., Compston, W., Trendall, A.F., Thorne, A.M., 1991. The age of the Fortescue Group, Hamersley Basin, Western Australia, from ion microprobe zircon U–Pb results. *Aust. J. Earth Sci.* 38, 261–281.
- Awramik, S.M., Buchheim, H.P., 2009. A giant, Late Archean lake system: the Meentheena Member (Tumbiana Formation; Fortescue Group), Western Australia. *Precambrian Res.* 174, 215–240.
- Bau, M., Alexander, B., 2006. Preservation of primary REE patterns without Ce anomaly during dolomitization of Mid-paleoproterozoic limestone and the potential re-establishment of marine anoxia immediately after the “Great Oxidation Event”. *S. Afr. J. Geol.* 109, 81–86.
- Blake, T.S., Buick, R., Brown, S.J.A., Barley, M.E., 2004. Geochronology of a Late Archean flood basalt province in the Pilbara Craton, Australia: constraints on basin evolution, volcanic and sedimentary accumulation, and continental drift rates. *Precambrian Res.* 133, 143–173.
- Bolhar, R., Van Kranendonk, M.J., 2007. A non-marine depositional setting for the northern Fortescue Group, Pilbara Craton, inferred from trace element geochemistry of stromatolitic carbonates. *Precambrian Res.* 155, 229–250.
- Buick, R., 1992. The antiquity of oxygenic photosynthesis: evidence from stromatolites in sulphate-deficient Archean lakes. *Science* 255, 74–77.
- Coffey, J.M., Walter, M.R., George, S.C., Hill, A.C., 2011. Paleontology and field observations of the ~2720 Ma Tumbiana Formation in the Northwest Pilbara, Western Australia. *Geological Survey of Western Australia, Record 2011/8.*, pp. 22.
- Dickson, J.A.D., 1965. A modified staining technique for carbonates in thin section. *Nature* 205, 587.
- Corkeron, M., Webb, G.E., Moulds, J., Grey, K., 2012. Discriminating stromatolite formation modes using rare earth element geochemistry: trapping and binding versus in situ precipitation of stromatolites from the Neoproterozoic Bitter Springs Formation, Northern Territory, Australia. *Precambrian Res.* 212–213, 194–206.
- Donaldson, J.A., 1976. Paleocology of Conophyton and associated stromatolites in the Precambrian Dismal Lake and Rae Groups. In: Walter, M.R. (Ed.), *Stromatolites*. Elsevier, pp. 523–534.
- Eigenbrode, J.L., Freeman, K.H., 2006. Late Archean rise of aerobic microbial ecosystems. *Proc. Nat. Acad. Sci.* 103, 15759–15764.
- Flannery, D.T., Hoshino, Y., George, S.C., Walter, M.R., 2012. Field observations relating to the c. 2740 Ma Mopoke Member, Kylene Formation, Fortescue Group, Pilbara region, Western Australia. *Geological Survey of Western Australia, Record 2012/8.*, pp. 1–12.
- Flannery, D.T., Walter, M.R., 2011. Archean tufted microbial mats and the great oxidation event: new insights into an ancient problem. *Aust. J. Earth Sci.* 59, 1–11.
- Glaessner, M.F., Preiss, W.V., Walter, M.R., 1969. Precambrian columnar stromatolites in Australia: morphological and stratigraphic analysis. *Science* 164, 1056–1058.
- Grotzinger, J.P., James, N.P., 2000. Precambrian carbonates: evolution of understanding. In: *Carbonate Sedimentation and Diagenesis in the Evolving Precambrian World*. SEPM (Society for Sedimentary Geology), pp. 3–20.
- Hofmann, H.J., 1969. Attributes of stromatolites, Geological Survey of Canada, Paper 39, p. 58.
- Holmes, J., Arrowsmith, C., Austin, W., Boyle, J., Fisher, E., Holme, R., Marshall, J., Oldfield, F., van der Post, K., 2010. Climate and atmospheric circulation changes over the past 1000 years reconstructed from oxygen isotopes in lake-sediment carbonate from Ireland. *Holocene* 20, 1105–1111.
- Jones, B., Renaut, R.W., Rosen, M.R., Ansdell, K.M., 2002. Coniform stromatolites from Geothermal Systems, North Island, New Zealand. *PALAIOS* 17, 84–103.
- Kamber, B.S., Greig, A., Collerson, K.D., 2005. A new estimate for the composition of weathered young upper continental crust from alluvial sediments, Queensland, Australia. *Geochim. Cosmochim. Acta* 69, 1041–1058.
- Kojan, C.J., Hickman, A.H., 1999. Late Archean Volcanism in the Kylene and Maddina Formations, Fortescue Group, west Pilbara. *Western Australia Geological Survey, Annual Review 1997–98.*, pp. 43–53.
- Kriewaldt, M., Ryan, G.R., 1967. *Western Australia Geological Survey 1:250,000 Geological Series, Pyramid, Explanatory Notes: Sheet SF/50-7.*, pp. 1–39.
- Lawrence, M.G., Greig, A., Collerson, K.D., Kamber, B.S., 2006. Direct quantification of rare earth element concentrations in natural waters by ICP-MS. *Appl. Geochem.* 21, 839–848.

- Lawrence, M.G., Kamber, B.S., 2006. The behaviour of the rare earth elements during estuarine mixing-revisited. *Mar. Chem.* 100, 147–161.
- Lepot, K., Benzerara, K., Brown, G.E., Philippot, P., 2008. Microbially influenced formation of 2,724-million-year-old stromatolites. *Nature Geosci.* 1, 118–121.
- Lindholm, R.C., Finkelman, R.B., 1972. Calcite staining: semiquantitative determination of ferrous iron. *J. Sediment. Res.* 42, 239–242.
- Lipple, L.S., 1975. Definitions of new and revised stratigraphic units of the eastern Pilbara region. Western Australia Geological Survey.
- Liu, W., Li, X., Zhang, L., An, Z., Xu, L., 2009. Evaluation of oxygen isotopes in carbonate as an indicator of lake evolution in arid areas: the modern Qinghai Lake, Qinghai-Tibet Plateau. *Chem. Geol.* 268, 126–136.
- Maslov, V.P., 1938. On the nature of the stromatolite Conophyton (Pre-Cambrian, Lower Tunguska river, Siberia). *Probl. Paleontol.* 4, 325–332.
- Nelson, D.R., 1998. Compilation of SHRIMP U–Pb zircon geochronology data. Western Australia Geological Survey, Record 1998/2.
- Nelson, D.R., 2001. Compilation of geochronology data, 2000.
- Nichols, G.J., Fisher, J.A., 2007. Processes, facies and architecture of fluvial distributary system deposits. *Sediment. Geol.* 195, 75–90.
- Packer, B.M., 1990. Sedimentology, Paleontology and Isotope-Geochemistry of Selected Formations in the 2.7 Billion-Year-Old Fortescue Group, Western Australia. University of California, Los Angeles (Ph.D. Thesis).
- Petroff, A.P., Sim, M.S., Maslov, A., Krupenin, M., Rothman, D.H., Bosak, T., 2010. Biophysical basis for the geometry of conical stromatolites. *Proc. Nat. Acad. Sci.* 107, 9956–9961.
- Platt, N.H., Wright, V.P., 2009. Lacustrine carbonates: facies models, facies distributions and hydrocarbon aspects. In: Anadón, P., Cabrera, L., Keltspp, K. (Eds.), *Lacustrine Facies Analysis*. Blackwell Publishing Ltd., pp. 57–74.
- Ricketts, B.D., Donaldson, J.A., 1979. Stone rosettes as indicators of ancient shorelines: examples from the Precambrian Belcher Group, Northwest Territories. *Can. J. Earth Sci.* 16, 1887–1891.
- Sakurai, R., Ito, M., Ueno, Y., Kitajima, K., Maruyama, S., 2005. Facies architecture and sequence-stratigraphic features of the Tumbiana Formation in the Pilbara Craton, northwestern Australia: implications for depositional environments of oxygenic stromatolites during the late Archean. *Precambrian Res.* 138, 255–273.
- Sanz-Montero, M.E., Rodriguez-Arnda, J.P., Garcia del Cura, M.A., 2009. Bioinduced precipitation of barite and celestite in dolomite microbialites: examples from Miocene lacustrine sequences in the Madrid and Duero Basins, Spain. *Sediment. Geol.* 222, 128–148.
- Schidlowski, M., Hayes, J.M., Kaplan, I.R., 1983. Isotopic inferences of ancient biochemistries: carbon, sulfur, hydrogen and nitrogen. In: Schopf, J.W. (Ed.), *Earth's Earliest Biosphere: Its Origin and Evolution*. Princeton University Press.
- Schopf, J.W., Sovietov, Y.K., 1976. Microfossils in Conophyton from the Soviet Union and their bearing on Precambrian biostratigraphy. *Science* 193, 143–146.
- Shepard, R.N., Sumner, D.Y., 2010. Undirected motility of filamentous cyanobacteria produces reticulate mats. *Geobiology* 8, 179–190.
- Smith, R.E., Perdrix, J.L., Parks, T.C., 1982. Burial metamorphism in the Hamersley Basin, Western Australia. *J. Petrol.* 23, 75–102.
- Thomazo, C., Ader, M., Farquhar, J., Philippot, P., 2009. Methanotrophs regulated atmospheric sulfur isotope anomalies during the Mesoarchean (Tumbiana Formation, Western Australia). *Earth Planet. Sci. Lett.* 279, 65–75.
- Thorne, A.M., Hickman, A.H., 1998. Geology of the Fortescue Group, Pilbara Craton (1:500 000 scale). In: Thorne, A.M., Trendall, A.F. (Eds.), *Geology of the Fortescue Group, Pilbara Craton, Western Australia*, vol. 144. Geological Survey of Western Australia, Bulletin, Plates 1a–1c.
- Thorne, A.M., Trendall, A.F., 2001. Geology of the Fortescue Group, Pilbara Craton, Western Australia. In: *Bulletin – Geological Survey of Western Australia* 144.
- Trendall, A.F., Blockley, J.G., 1970. The iron formations of the Precambrian Hamersley Group, Western Australia, with special reference to the associated crocidolite. In: *Bulletin – Geological Survey of Western Australia* 119., pp. 366.
- Van Kranendonk, M.J., Philippot, P., Lepot, K., 2006. The Pilbara drilling project: c. 2.72 Ga Tumbiana Formation and c. 3.49 Ga Dresser Formation, Pilbara Craton, Western Australia. Western Australia Geological Survey, Record 2006/14., pp. 25.
- Veizer, J., Hoefs, J., Ridler, R.H., Jensen, L.S., Lowe, D.R., 1989. Geochemistry of Precambrian carbonates: I. Archean hydrothermal systems. *Geochim. Cosmochim. Acta* 53, 845–857.
- Walter, M.R., 1972. Stromatolites and the biostratigraphy of the Australian Precambrian and Cambrian. *Spec. Pap. Palaeontol.* 11, 256.
- Walter, M.R., 1983. Archean stromatolites; evidence of the Earth's earliest benthos. In: Schopf, J.W. (Ed.), *Earth's Earliest Biosphere: Its Origin and Evolution*. Princeton Univ. Press, Princeton.
- Walter, M.R., Bauld, J., Brock, T.D., 1976. Microbiology and morphogenesis of columnar stromatolites (Conophyton, Vacerrilla) from hot springs in Yellowstone National Park. In: Walter, M.R. (Ed.), *Stromatolites*. Elsevier Sci. Publ. Co., Amsterdam, pp. 273–310.
- Webb, G.E., Kamber, B.S., 2000. Rare earth elements in Holocene reefal microbialites: a new shallow seawater proxy. *Geochim. Cosmochim. Acta* 64, 1557–1565.